

Four-body calculation of ${}^2\text{H}(d,p){}^3\text{H}$ and ${}^2\text{H}(d,n){}^3\text{He}$ reactions above breakup threshold

A. Deltuva*

Institute of Theoretical Physics and Astronomy, Vilnius University, Saulėtekio al. 3, LT-10222 Vilnius, Lithuania

A. C. Fonseca

Centro de Física Nuclear da Universidade de Lisboa, P-1649-003 Lisboa, Portugal

(Received September 10, 2018)

Nucleon transfer reactions in deuteron-deuteron collisions at energies above the three- and four-body breakup threshold are described using exact four-body equations for transition operators that are solved in the momentum-space framework. Differential cross sections, analyzing powers, polarizations, and spin transfer coefficients are obtained using realistic two-nucleon potentials and including the Coulomb repulsion between protons. Overall good agreement between predictions and experimental data is found. Most remarkable discrepancies are seen around the minima of the differential cross section at higher energies and in the outgoing nucleon polarization at lower energies.

PACS numbers: 21.30.-x, 21.45.-v, 24.70.+s, 25.10.+s

I. INTRODUCTION

In the last 10 years significant progress has taken place in exact ab initio calculations of two-cluster scattering in the four-nucleon system, both below [1–9] and above [10–17] the breakup threshold. In the case of multichannel reactions, i.e., processes with open rearrangements and/or breakup channels, the most advanced calculations were performed by solving the Alt, Grassberger, and Sandhas (AGS) equations [18, 19] for the four-particle transition operators in the momentum-space framework. Realistic nucleon-nucleon (NN) force models were included as well as the Coulomb interaction between protons, and the effective three- and four-nucleon ($3N$ and $4N$) forces through explicit Δ -isobar excitation. Comparing the predictions with the available experimental data one could say that the realistic force models provide a satisfactory explanation of the cross sections and spin observables over a broad energy regime up to about 30 MeV, reproducing the proper energy dependence and changes in shape of the observables as the energy rises. Agreement with data can be in some cases paradigmatic, given the complex structure of some observables that display several maxima and minima, a feature that is not so often observed in three-nucleon data. However, there are also a few disagreements with the data whose magnitude is sensitive to the force model used and may serve as a fertile ground for the investigation of nuclear interactions. Still missing in this study is the extension of the nucleon transfer reactions ${}^2\text{H}(d,p){}^3\text{H}$ and ${}^2\text{H}(d,n){}^3\text{He}$ initiated by deuteron-deuteron collisions at energies well above the breakup threshold where the existing differential cross section and analyzing power data [20–32] show a complicated structure involving several maxima and minima that change with the energy. Therefore in

the present manuscript we aim to investigate ${}^2\text{H}(d,p){}^3\text{H}$ and ${}^2\text{H}(d,n){}^3\text{He}$ reactions up to about 25 MeV deuteron beam energy.

In Sec. II we present the theoretical framework. Differential cross section and spin observable results are reported in Sec. III and a summary is presented in Sec. IV.

II. THEORY

The four-particle collision process is described by the exact AGS equations [18, 19] for the transition operators $\mathcal{U}_{\beta\alpha}$ whose components are labeled according to the chains of partitions. Given that in the isospin formalism neutrons and protons are treated as identical particles, there are only two chains of partitions that can be distinguished by the two-cluster partitions, one ($\alpha = 1$) being of the $3+1$ type, i.e., $(12,3)4$, and another ($\alpha = 2$) being of the $2+2$ type, i.e., $(12)(34)$. For nucleon-trinucleon scattering in previous works we solved the symmetrized AGS equations for $\mathcal{U}_{\beta 1}$, but for reactions initiated by two deuterons, transition operators $\mathcal{U}_{\beta 2}$ are required. In both cases the AGS equations share the same kernel but differ in the driving term. Thus, in the present work we solve the integral equations

$$\mathcal{U}_{12} = (G_0 t G_0)^{-1} - P_{34} U_1 G_0 t G_0 \mathcal{U}_{12} + U_2 G_0 t G_0 \mathcal{U}_{22}, \quad (1a)$$

$$\mathcal{U}_{22} = (1 - P_{34}) U_1 G_0 t G_0 \mathcal{U}_{12}. \quad (1b)$$

Here t is the two-nucleon transition matrix, U_1 and U_2 are the transition operators for the $1+3$ and $2+2$ subsystems, P_{34} is the permutation operator of particles 3 and 4, and $G_0 = (E + i\varepsilon - H_0)^{-1}$ is the free four-particle resolvent at the available energy E , whereas H_0 is the free Hamiltonian. Although the physical scattering process corresponds to $\varepsilon \rightarrow +0$, the complex energy method uses a finite ε value when solving the AGS equations numerically. The physical scattering amplitudes are then

* arnoldas.deltuva@tfai.vu.lt

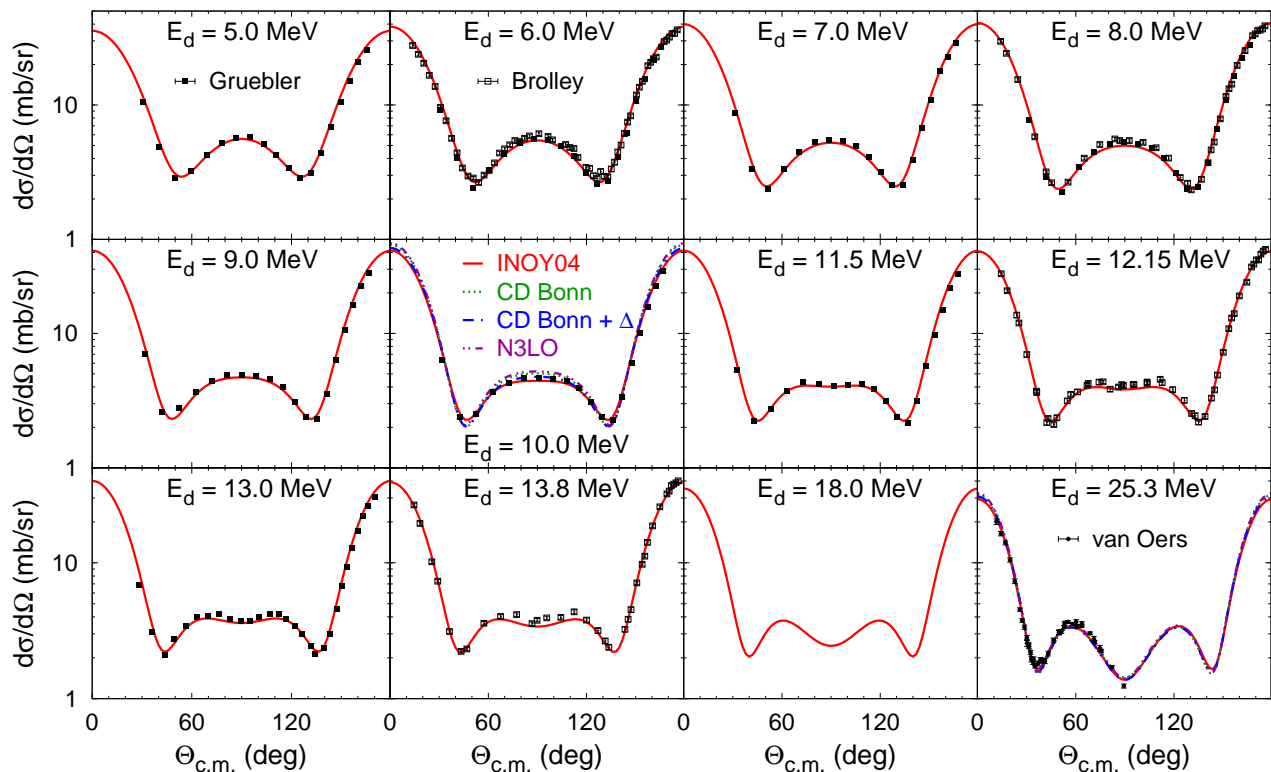


FIG. 1. (Color online) Differential cross section for the ${}^2\text{H}(d,p){}^3\text{H}$ reaction as a function of the c.m. scattering angle at deuteron beam energies ranging from 5.0 to 25.3 MeV. Results are obtained using the INOY04 potential (solid curves), and, at 10.0 and 25.3 MeV, also the CD Bonn + Δ (dashed-dotted curves), CD Bonn (dotted curves), and N3LO (double-dotted-dashed curves) potentials. Experimental data are from Refs. [20, 21] (\blacksquare), [22] (\square), and [23] (\bullet).

obtained by extrapolating finite ε results to the $\varepsilon \rightarrow +0$ limit. The extrapolation procedure, as well as the special method for integrals with quasi-singularities encountered when solving Eqs. (1), is described in detail in our previous works [10, 13, 33].

The pp Coulomb force is included using the method of screening and renormalization [4, 34] where the screening radius $R = 12$ to 16 fm is found to be sufficient to achieve convergence for the Coulomb-distorted short-range part of the amplitude. The obtained results are well converged with respect to the partial-wave expansion. When solving Eqs. (1) we take into account isospin-singlet $2N$ partial waves with total angular momentum $j_x \leq 4$ and isospin-triplet $2N$ partial waves with orbital angular momentum $l_x \leq 7$, $3N$ partial waves with spectator orbital angular momentum $l_y \leq 7$ and total angular momentum $J \leq \frac{13}{2}$, and $4N$ partial waves with 1+3 and 2+2 orbital angular momentum $l_z \leq 8$. Initial and final deuteron-deuteron states with relative orbital angular momentum $L \leq 6$ are sufficient for the calculation of observables except at the 25.3 MeV beam energy where we take into account also the states up to $L \leq 8$ that yield a small but visible contribution.

III. RESULTS

The scattering of two deuterons, as compared to nucleon-trinucleon collisions, is more challenging from the computational point of view but also interesting physicswise. Since deuterons are loosely bound and spatially large objects, their collision involves more partial waves and gives rise to much higher breakup cross sections than encountered in other $4N$ reactions initiated by nucleons and trinucleons.

The threshold for one (two) deuteron breakup corresponds to the deuteron beam energy $E_d = 4.45$ MeV (8.90 MeV). We calculate differential cross sections $d\sigma/d\Omega$ and various spin observables for ${}^2\text{H}(d,p){}^3\text{H}$ and ${}^2\text{H}(d,n){}^3\text{He}$ reactions as functions of the nucleon center-of-mass (c.m.) scattering angle $\Theta_{\text{c.m.}}$ at E_d ranging from 5.0 to 25.3 MeV. At all considered energies the results are obtained using the realistic inside-nonlocal outside-Yukawa (INOY04) potential of Doleschall [2, 35] since it nearly reproduces the experimental values of the ${}^3\text{He}$ and ${}^3\text{H}$ binding energies with no additional $3N$ force. To investigate the dependence of the results on the interaction model, at $E_d = 10$ and 25.3 MeV, we also show the predictions obtained with other high-precision NN potentials. These are the chiral effective field theory po-

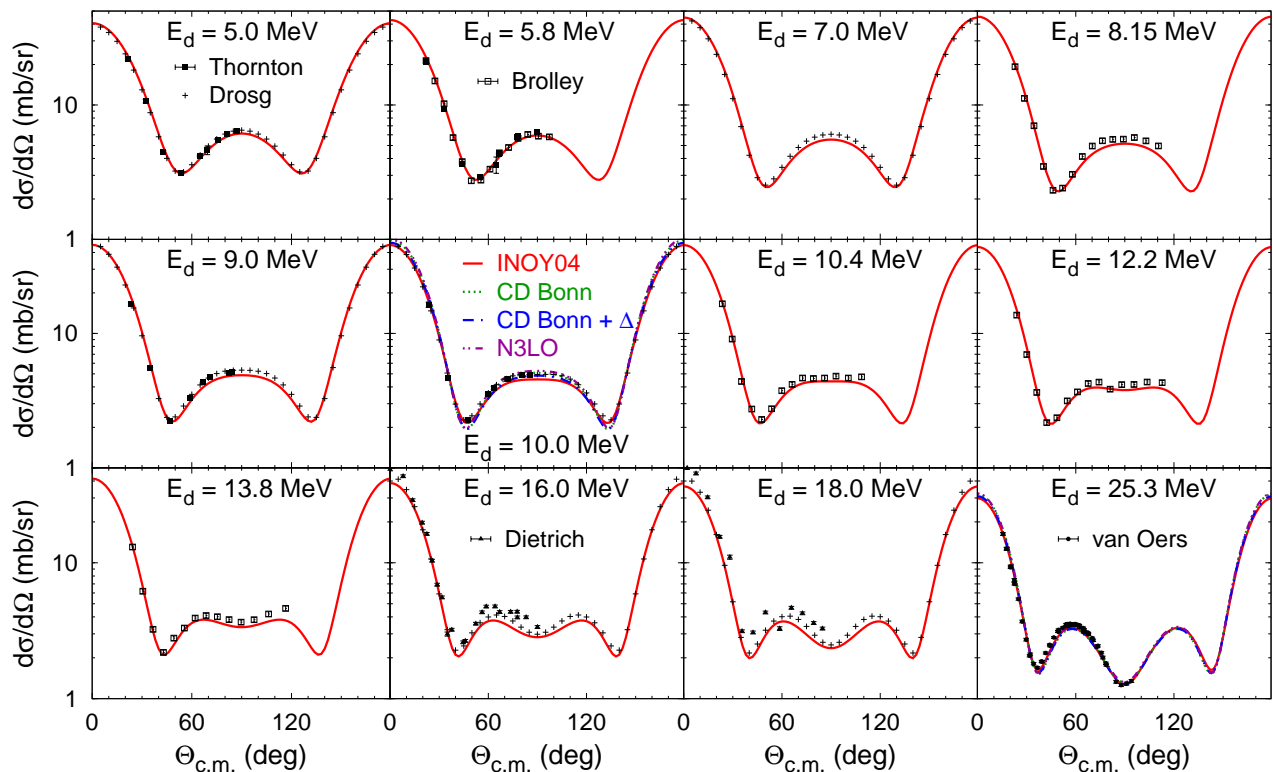


FIG. 2. (Color online) Differential cross section for the ${}^2\text{H}(d,n){}^3\text{He}$ reaction as a function of the c.m. scattering angle at deuteron beam energies ranging from 5.0 to 25.3 MeV. Curves are as in Fig. 1. Experimental data are from Refs. [24] (■), [25] (+), [22] (□), [26] (▲), and [23] (●).

tential at next-to-next-to-next-to-leading order (N3LO) [36], the charge-dependent Bonn potential (CD Bonn) [37], and its extension CD Bonn + Δ [38] that explicitly includes the excitation of a nucleon to a Δ isobar. This mechanism generates effective $3N$ and $4N$ forces that are mutually consistent but quantitatively still insufficient to reproduce $3N$ and $4N$ binding energies, although they reduce the discrepancy [39]. The predictions for ${}^3\text{He}$ and ${}^3\text{H}$ binding energies for all employed force models are collected in Table I.

	$B({}^3\text{H})$	$B({}^3\text{He})$
N3LO	7.85	7.13
CD Bonn	8.00	7.26
CD Bonn + Δ	8.28	7.53
INOY04	8.49	7.73
Experiment	8.48	7.72

TABLE I. ${}^3\text{H}$ and ${}^3\text{He}$ binding energies (in MeV) for different NN potentials.

In Figs. 1 and 2 we show the differential cross sections for the transfer reactions ${}^2\text{H}(d,p){}^3\text{H}$ and ${}^2\text{H}(d,n){}^3\text{He}$, respectively. Due to identity of the two deuterons this observable is symmetric with respect to $\Theta_{\text{c.m.}} = 90^\circ$ and is

peaked in the forward and backward directions. As the energy rises, the local maximum of $d\sigma/d\Omega$ at $\Theta_{\text{c.m.}} = 90^\circ$ evolves into a local minimum between two local maxima at about 60° and 120° . Over the whole energy and angular regime the INOY04 results closely follow the experimental data [20–24], only slightly underpredicting some of them around $\Theta_{\text{c.m.}} = 90^\circ$. The ${}^2\text{H}(d,n){}^3\text{He}$ data from Ref. [26] are obviously wrong as they are inconsistent with the global evaluation [25]. The sensitivity to the NN force model is visible at $E_d = 10$ MeV, where it can reach 15%, but decreases with the energy, becoming insignificant at $E_d = 25.3$ MeV. As at very low energies [5], the predictions roughly scale with the trinucleon binding energy.

The deuteron vector analyzing power iT_{11} and tensor analyzing powers T_{20} , T_{21} , and T_{22} are shown in Figs. 3 and 4 for the same transfer reactions up to $E_d = 13$ MeV and compared with the experimental data [20, 21, 27, 28]; we are not aware of experimental data at higher energies. These observables do not exhibit any symmetry with respect to $\Theta_{\text{c.m.}} = 90^\circ$ as only the beam deuteron is polarized. We observe a few small discrepancies between predictions and data, mostly for iT_{11} and T_{20} at $\Theta_{\text{c.m.}} < 60^\circ$ in ${}^2\text{H}(d,p){}^3\text{H}$, but the overall agreement with the data is impressive given the complicated angular dependence of the analyzing powers. The sensitivity to the NN force

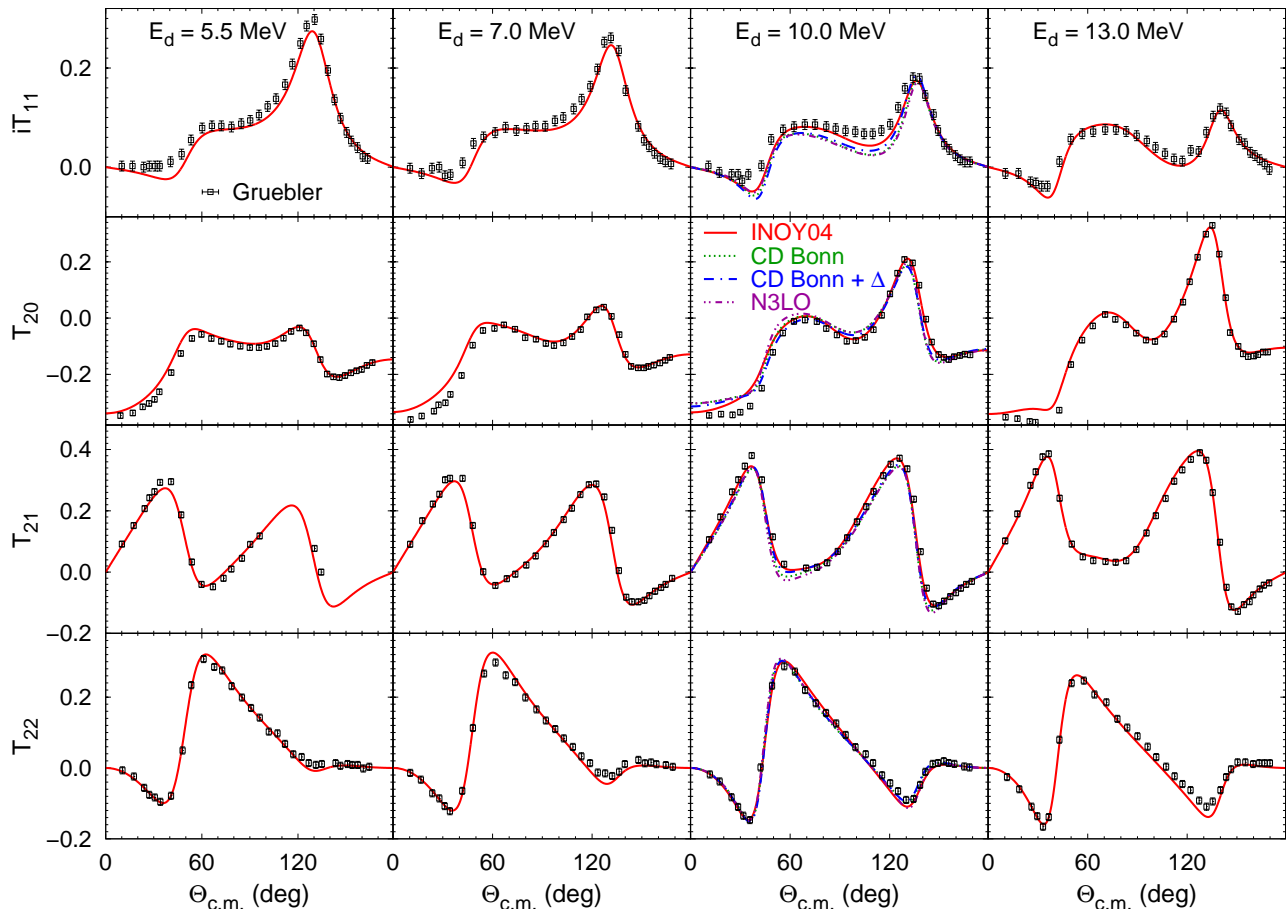


FIG. 3. (Color online) Deuteron analyzing powers for the ${}^2\text{H}(d,p){}^3\text{H}$ reaction at $E_d = 5.5, 7.0, 10.0,$ and 13.0 MeV. Curves are as in Fig. 1. Experimental data are from Ref. [21].

model is again visible, especially for iT_{11} , but shows no clear correlation with the trinucleon binding energy.

The polarization P_y of the outgoing nucleon for ${}^2\text{H}(d,p){}^3\text{H}$ and ${}^2\text{H}(d,n){}^3\text{He}$ reactions is presented in Fig. 5. This observable is antisymmetric with respect to $\Theta_{\text{c.m.}} = 90^\circ$; hence we show only the angular regime $\Theta_{\text{c.m.}} < 105^\circ$ for E_d up to 14 MeV where the experimental data [29, 30] are available. This observable exhibits a peak near $\Theta_{\text{c.m.}} = 45^\circ$ whose height is well reproduced by the calculations with the INOY04 potential but the position is shifted to larger angles by about 2 to 8 degrees; this shift is more pronounced at lower beam energies. The sensitivity to the NN potential at $E_d = 10$ MeV is comparable to the one observed for analyzing powers, but becomes significantly larger at lower energies. This is illustrated by the CD Bonn predictions at $E_d = 6$ MeV and is consistent with the strong model dependence found in Ref. [40] at $E_d = 3$ MeV. We note that P_y is equal to the nucleon analyzing power A_y in the respective time reversed reactions ${}^3\text{H}(p,d){}^2\text{H}$ and ${}^3\text{He}(n,d){}^2\text{H}$ at the same energy E . Given that A_y in low-energy nucleon-trinucleon scattering shows sizable discrepancies between predictions and data for both elastic and charge-

exchange reactions [16], some discrepancies for A_y in the coupled nucleon transfer reactions are expected. A similar conclusion can also be drawn regarding the NN force sensitivity in all coupled reactions.

Measurement of double-polarization observables is highly complicated; thus, the corresponding data are quite scarce. We are aware of only two experiments measuring the angular dependence of deuteron-to-nucleon polarization transfer coefficients, i.e., $K_x^{x'}$, $K_z^{z'}$, $K_x^{y'}$, $K_z^{y'}$, and $K_y^{y'}$ in the ${}^2\text{H}(\vec{d}, \vec{n}){}^3\text{He}$ reaction at $E_d = 10$ MeV [31], and $K_x^{x'}$, $K_z^{x'}$, $K_y^{y'}$, $K_{xx}^{y'}$, $K_{yy}^{y'}$, $K_{zz}^{y'}$, and $K_{xz}^{y'}$ in the ${}^2\text{H}(\vec{d}, \vec{p}){}^3\text{H}$ reaction at $E_d = 10.15$ MeV [32]. The former set is already analyzed in our earlier work [14]. Despite the very complex angular dependence of deuteron-to-neutron polarization transfer coefficients having up to six local extrema, a good agreement between theory and experiment and little sensitivity to the NN force model are found. A similar situation holds also for the ${}^2\text{H}(\vec{d}, \vec{p}){}^3\text{H}$ reaction at $E_d = 10.15$ MeV. We present our predictions using the INOY04 and N3LO potentials in Fig. 6. There are only four data points for each observable, and almost all of them lie on theoretical curves,

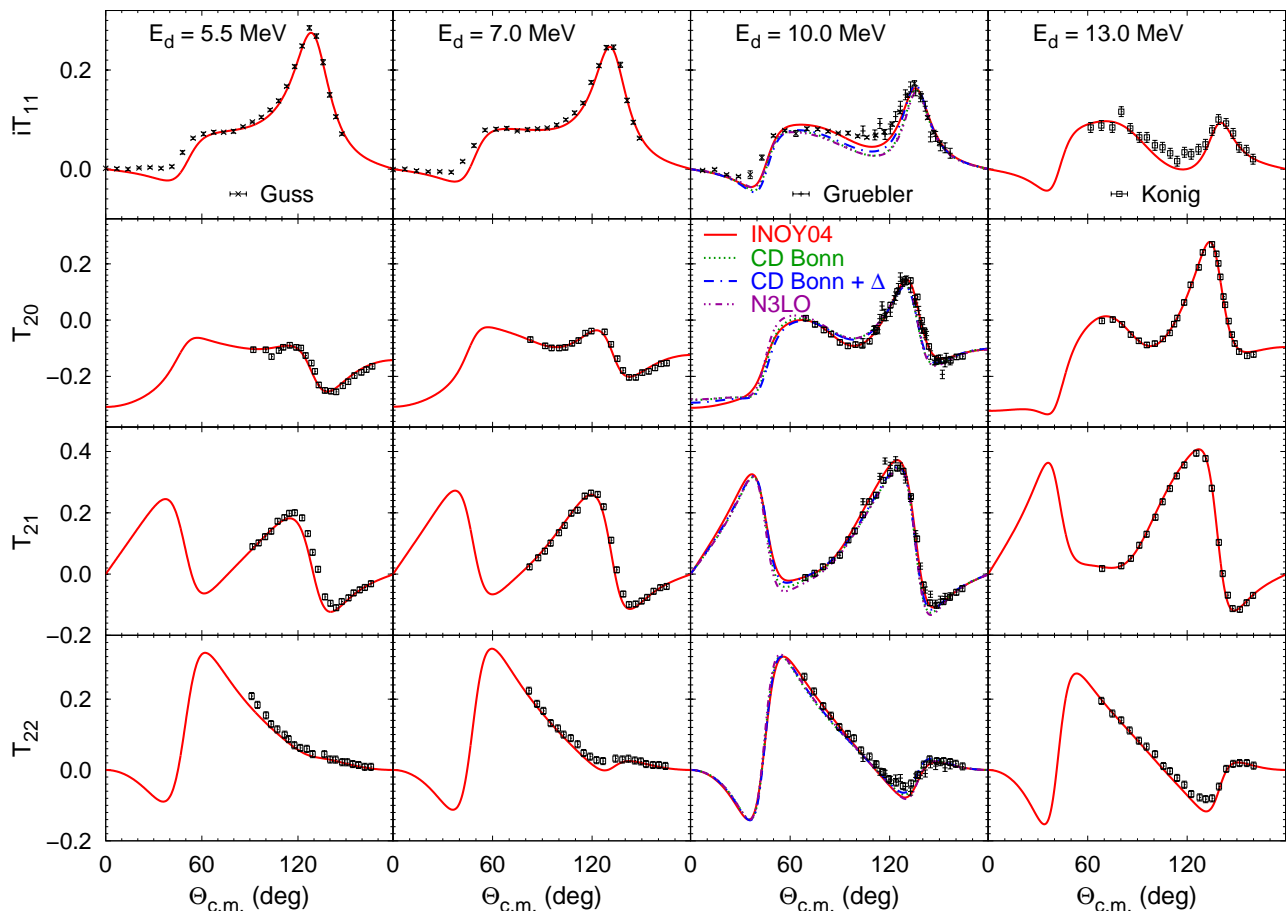


FIG. 4. (Color online) Deuteron analyzing powers for the ${}^2\text{H}(d, n){}^3\text{He}$ reaction at $E_d = 5.5, 7.0, 10.0,$ and 13.0 MeV. Curves are as in Fig. 1. Experimental data are from Refs. [27] (\times), [20] ($+$), and [28] (\square)

the exceptions being one or two points for K_{yy}' and K_{xz}' having quite large error bars. Thus, one may conclude that the overall description of polarization transfer data for both ${}^2\text{H}(\vec{d}, \vec{n}){}^3\text{He}$ and ${}^2\text{H}(\vec{d}, \vec{p}){}^3\text{H}$ reactions is quite satisfactory.

Finally, in Fig. 7 we show the energy dependence of the total cross section (integrated over the scattering angle) for both transfer reactions and the sum of the three- and four-cluster breakup. An explicit calculation of the breakup amplitudes is highly demanding, but the total breakup cross section is obtained as the difference between the full and all two-cluster channels cross sections, applying optical theorem for amplitudes calculated with a sufficiently large Coulomb screening radius [13]. The comparison with data for the transfer cross sections is reasonably good as could be expected from the comparison of differential cross sections in Figs. 1 and 2. We are not aware of total breakup cross section data. We predict a rapid increase of the breakup cross section at low energies, exceeding the transfer cross sections around $E_d = 9$ MeV and becoming the most important inelastic channel. For example, at $E_d = 25.3$ MeV the breakup cross section reaches 287 mb, more than 6 times larger than

each of the transfer cross sections. In the same figure we show the total proton-deuteron breakup cross section as a function of the proton beam energy. This reaction has a lower threshold, but beyond 12 MeV the deuteron-deuteron breakup cross section exceeds the one for the proton-deuteron breakup, reaching a factor of 2 between them at 25 MeV. It is interesting to note that this factor of two at higher energies may be simply conjectured as resulting from the sum of projectile deuteron breakup and target deuteron breakup, given the symmetry of the deuterons in the entrance channel.

IV. SUMMARY

In the present manuscript we show the results of our numerical calculations aiming to describe the world data for both transfer reactions, ${}^2\text{H}(d, p){}^3\text{H}$ and ${}^2\text{H}(d, n){}^3\text{He}$, in the energy region above the three- and four-body breakup threshold, and present predictions for the total deuteron-deuteron breakup cross section up to $E_d = 25$ MeV. The calculations include realistic NN force models and the Coulomb interaction between protons. Given

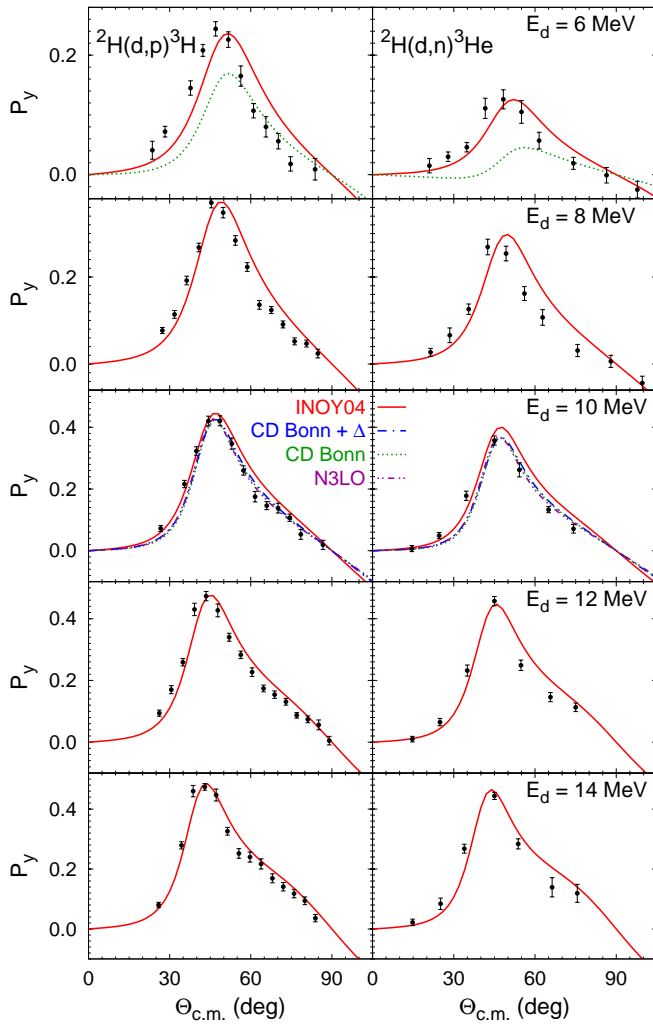


FIG. 5. Outgoing nucleon polarization of the ${}^2\text{H}(d,p){}^3\text{H}$ (left) and ${}^2\text{H}(d,n){}^3\text{He}$ (right) transfer reactions at deuteron beam energies ranging from 6 to 14 MeV. Curves are as in Fig. 1. Experimental data are from Refs. [29, 30] for the ${}^2\text{H}(d,p){}^3\text{H}$ and ${}^2\text{H}(d,n){}^3\text{He}$ reactions, respectively.

the large size of the deuteron, elastic scattering of two deuterons can be expected to be peripheral and display little sensitivity to the choice of NN interaction. Nevertheless this argumentation is not completely valid for the transfer reactions where threshold positions depend on the NN force. Furthermore, due to the weak binding, deuteron-deuteron reactions are more demanding computationally as they involve more partial waves and give rise to higher breakup cross sections. In contrast to nucleon-trinucleon reactions, given the symmetry of the two deuterons in the initial channel, only states that are symmetric under the exchange of the two deuterons contribute the observables which by itself curtails the number of combinations through which the NN force affects the transfer observables. Another aspect in favor of deuteron-deuteron reactions relative to nucleon-

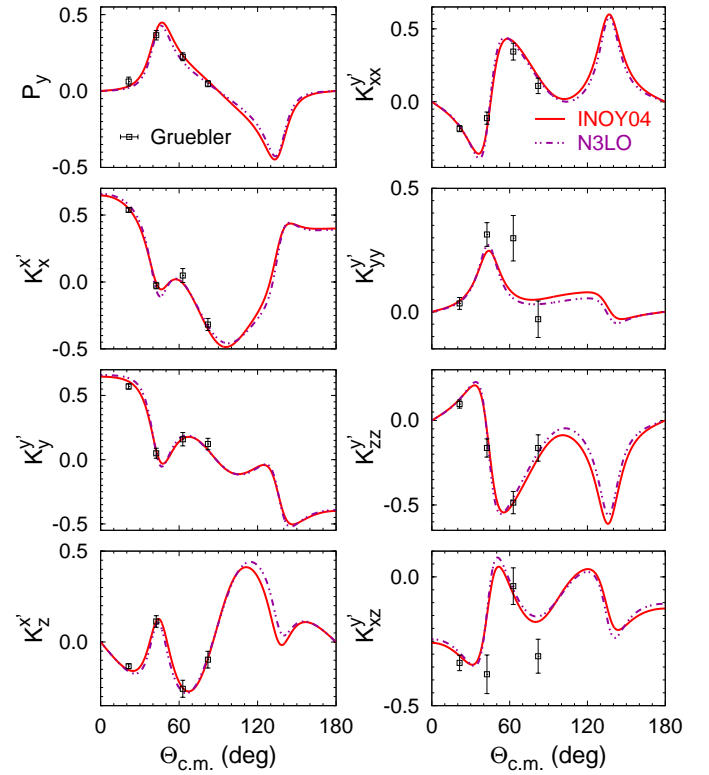


FIG. 6. Outgoing proton polarization P_y and deuteron-to-proton polarization transfer coefficients for the ${}^2\text{H}(d,p){}^3\text{H}$ reaction at 10.15 MeV deuteron energy. Curves are as in Fig. 1. Experimental data are from Ref. [32].

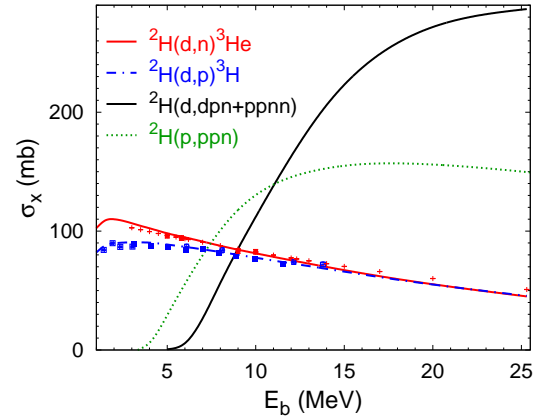


FIG. 7. Total cross sections for transfer and breakup reactions in deuteron-deuteron collisions as functions of the beam energy. In addition, results for the proton-deuteron breakup are represented by the dotted curve. Experimental data for transfer reactions are from Refs. [20–22, 24, 25].

trinucleon is that the threshold is well above the region where the four-nucleon system displays a complex structure of resonances. Nevertheless, these features do not allow for a reasonable simplification of the AGS equations (1), as all the terms are important and cannot be neglected.

This being said one cannot avoid concluding that the results we obtain provide a very impressive description of the world data for the ${}^2\text{H}(d, p){}^3\text{H}$ and ${}^2\text{H}(d, n){}^3\text{He}$ reactions up to $E_d = 25$ MeV. Given the complex structure of these data, not seen in nucleon-trinucleon or nucleon-deuteron scattering, discrepancies are very few and limited to a few observables such as iT_{11} and P_y and small angular regions, in spite of the large number of maxima and minima displayed by the data. Also double-polarization experiments are well described by the calculations.

With this work we have completed the study of all possible two-cluster reactions in the four-nucleon system

using realistic pairwise potentials, and have brought the four-nucleon scattering problem to the same degree of development that three-nucleon scattering obtained already a number of years ago. Further progress is still needed to calculate the breakup observables, but the lack of accurate breakup data makes the effort superfluous for now. In a recent article [41] we reviewed our previous work and suggested that the best theoretical laboratory to study NN force models is in fact the low-energy region where there are a number of four-nucleon resonances in both $T = 0$ and $T = 1$ total isospin configurations. Although four-nucleon calculations are more time consuming and pose greater numerical challenges, one finds a greater sensitivity to NN force models as compared to the three-nucleon system.

The authors thank M. Drosg for the discussion of experimental data. A.D. acknowledges partial support from Lietuvos Mokslo Taryba (Research Council of Lithuania) under Project. No. KEL-15018.

-
- [1] M. Viviani, A. Kievsky, S. Rosati, E. A. George, and L. D. Knutson, Phys. Rev. Lett. **86**, 3739 (2001).
- [2] R. Lazauskas and J. Carbonell, Phys. Rev. C **70**, 044002 (2004).
- [3] A. Deltuva and A. C. Fonseca, Phys. Rev. C **75**, 014005 (2007).
- [4] A. Deltuva and A. C. Fonseca, Phys. Rev. Lett. **98**, 162502 (2007).
- [5] A. Deltuva and A. C. Fonseca, Phys. Rev. C **76**, 021001(R) (2007).
- [6] A. Kievsky, S. Rosati, M. Viviani, L. E. Marcucci, and L. Girlanda, J. Phys. G **35**, 063101 (2008).
- [7] R. Lazauskas, Phys. Rev. C **79**, 054007 (2009).
- [8] M. Viviani, R. Schiavilla, L. Girlanda, A. Kievsky, and L. E. Marcucci, Phys. Rev. C **82**, 044001 (2010).
- [9] M. Viviani, L. Girlanda, A. Kievsky, and L. E. Marcucci, Phys. Rev. Lett. **111**, 172302 (2013).
- [10] A. Deltuva and A. C. Fonseca, Phys. Rev. C **86**, 011001(R) (2012).
- [11] A. Deltuva and A. C. Fonseca, Phys. Rev. C **87**, 054002 (2013).
- [12] A. Deltuva and A. C. Fonseca, Phys. Rev. Lett. **113**, 102502 (2014).
- [13] A. Deltuva and A. C. Fonseca, Phys. Rev. C **90**, 044002 (2014).
- [14] A. Deltuva and A. Fonseca, Phys. Lett. B **742**, 285 (2015).
- [15] R. Lazauskas, Phys. Rev. C **91**, 041001 (2015).
- [16] A. Deltuva and A. C. Fonseca, Phys. Rev. C **91**, 034001 (2015).
- [17] A. Deltuva and A. C. Fonseca, Phys. Rev. C **92**, 024001 (2015).
- [18] P. Grassberger and W. Sandhas, Nucl. Phys. **B2**, 181 (1967).
- [19] E. O. Alt, P. Grassberger, and W. Sandhas, JINR report **E4-6688**, 1 (1972).
- [20] W. Grüebler, V. König, P. A. Schmelzbach, R. Risler, R. E. White, and P. Marmier, Nucl. Phys. A **193**, 129 (1972).
- [21] W. Grüebler, V. König, P. A. Schmelzbach, B. Jenny, and J. Vybiral, Nucl. Phys. A **369**, 381 (1981).
- [22] J. E. Brolley, T. M. Putnam, and L. Rosen, Phys. Rev. **107**, 820 (1957).
- [23] W. T. H. Van Oers and K. W. Brockman Jr., Nucl. Phys. **48**, 625 (1963).
- [24] S. Thornton, Nucl. Phys. A **136**, 25 (1969).
- [25] M. Drosg and N. Otuka, INDC report INDC-0019, 1 (2015); in EXFOR Database (NNDC, Brookhaven, 2015).
- [26] F. Dietrich, E. Adelberger, and W. Meyerhof, Nucl. Phys. A **184**, 449 (1972).
- [27] P. Guss, K. Murphy, R. Byrd, C. Floyd, S. Wender, R. Walter, T. Clegg, and W. Wylie, Nucl. Phys. A **395**, 1 (1983).
- [28] V. König, W. Grüebler, R. A. Hardekopf, B. Jenny, R. Risler, H. Brgi, P. Schmelzbach, and R. White, Nucl. Phys. A **331**, 1 (1979).
- [29] R. Hardekopf, P. Lisowski, T. Rhea, R. Walter, and T. Clegg, Nucl. Phys. A **191**, 468 (1972).
- [30] G. Spalek, R. Hardekopf, J. T. Jr., T. Stambach, and R. Walter, Nucl. Phys. A **191**, 449 (1972).
- [31] G. Salzman, G. G. Ohlsen, J. Martin, J. Jarmer, and T. Donoghue, Nucl. Phys. A **222**, 512 (1974).
- [32] W. Grüebler, R. A. Hardekopf, D. D. Armstrong, and P. W. Keaton, Nucl. Phys. A **230**, 353 (1974).
- [33] J. Carbonell, A. Deltuva, A. Fonseca, and R. Lazauskas, Progress in Particle and Nuclear Physics **74**, 55 (2014).
- [34] E. O. Alt and W. Sandhas, Phys. Rev. C **21**, 1733 (1980).
- [35] P. Doleschall, Phys. Rev. C **69**, 054001 (2004).
- [36] D. R. Entem and R. Machleidt, Phys. Rev. C **68**, 041001(R) (2003).
- [37] R. Machleidt, Phys. Rev. C **63**, 024001 (2001).
- [38] A. Deltuva, R. Machleidt, and P. U. Sauer, Phys. Rev. C **68**, 024005 (2003).
- [39] A. Deltuva, A. C. Fonseca, and P. U. Sauer, Phys. Lett. B **660**, 471 (2008).
- [40] A. Deltuva and A. C. Fonseca, Phys. Rev. C **81**, 054002 (2010).

- [41] A. C. Fonseca and A. Deltuva, Few-Body Syst. submitted, (2016).